Lab on a Chip

Accepted Manuscript

ROYAL SOCIETY OF CHEMISTRY

www.rsc.org/loc

Journal Name

RSCPublishing

ARTICLE

A Cyclically Actuated Electrolytic Drug Delivery Device

Cite this: DOI: 10.1039/xoxxoooooox

Ying Yi,[a] Ulrich Buttner,[a] and Ian G. Foulds[b]

Received ooth January 2012,
Accepted ooth January 2012

DOI: 10.1039/xoxxoooooox

www.rsc.org/

This work, focusing on an implantable drug delivery system, presents the first prototype electrolytic pump that combines a catalytic reformer and a cyclically actuated mode. These features improve the release performance and extend the lifetime of the device. Using our platinum (Pt) coated carbon fiber mesh that acts as a catalytic reforming element; the cyclical mode is improved because the faster recombination rate allows for a shorter cycling time for drug delivery. Another feature of our device is that is using a solid drug in reservoir (SDR) approach, which allows small amounts of solid drug to be dissolved in human liquid, forming a reproducible drug solution for long-term therapies. We have conducted proof-of-principle drug delivery studies using such an electrolytic-pump and solvent blue 38 as the drug substitute. These tests, demonstrate power-controlled and pulsatile release profiles of the chemical substance, as well as the feasibility of this device. A drug delivery rate of 11.44 ± 0.56 ug/min was achieved by using an input power of 4 mW for multiple pulses, which indicates the stability of our system.

1. Introduction

Therapeutic effect is affected by drug concentration at the disease site. Dosing must be precisely controlled, especially for potent drugs, because immediate release or overdose may lead to does-related side effects.[1] Unfortunately, conventional drug delivery methods, which include oral ingestions, eye drops, and injections, usually do not exhibit targeted and controlled drug release, thereby increasing the potential for toxicity. In addition, conventional treatments require large overdoses to reach therapeutic levels, because more than 95% of the applied medication is obstructed by physiological barriers.[2] As for the drug itself, mixing of many unnecessary chemicals (such as flavoring agents, binders, and carriers) further reduce the medication efficiency. For treating chronic diseases, such as diabetes, frequent injections also bring substantial discomfort and pain to patients.

In contrast to typical drug therapy systems, newly emerged implantable drug delivery devices are capable of providing controllable and precisely targeted dosing, demonstrating feasible applications for treating chronic diseases, such as proliferative diabetic retinopathy,[3] and brain tumors.[4] According to the patients' requirements, once the devices are implanted, the drug can be released for a short time (several days) or over extended periods (months or even years); extra surgical interventions are not needed, reducing medical cost and patients' pains. Localized and controlled drug release could not only optimize the medication efficiency,[5] but it also maintains the desired concentration within the effective therapeutic range. Moreover, implantable devices provide possible solutions for new pharmaceutical agents, such as biologics, biosimilars and other small molecules, which are not easily administered by conventional delivery methods.[1]

Among the previously reported implantable drug delivery devices, some of them are implemented using polymers with specific physical or chemical characteristics,[6] such as biodegradability,[7] sensitivity to pH, or temperature.[8] The actuation of such devices mainly relies on diffusion or osmotic pressure; therefore, these methods are functioning as "passively controlled" delivery, and accordingly, the dosing is not flexible over the release lifetime. Whereas delivering a well-defined dose of drug via an external on-demand actuation exhibits more advantages over passively controlled drug release, such as flexible dosing, an adjustable release rate and a controllable drug concentration. To some extent, Microfluidic-based drug delivery devices provide potential platforms to achieve these purposes.

During the past two decades, microfluidic devices have been developed and are able to afford a variety of novel biomedical and lab-on-a-chip applications due to their structural, mechanical, and electronic features. Microfluidics provides various platforms for microsystems, such as tissue engineering,[9] biological analysis chips[10] and controlled drug delivery.[11-13] In general, microfluidics-based drug delivery systems require two categories of actuation to displace drug solution: direct electro-mechanical actuation and non-mechanical actuation. The actuation mechanisms based on direct electro-mechanical force transduction include electrostatic,[14] piezoelectric,[15] and electromagnetic.[16] These methods provide high drug release rates (>10 μL/min); however compared to their non-electro-mechanical counterparts (e.g. electrochemical[17] and osmotic systems.[18-19]), they require larger sizes, more complicated structures and higher power consumption.

More recently, electrolytic-pump-based drug delivery systems have been investigated among the non-mechanical devices due to their precise flow control, stable pumping performance, appropriate flow rate, low heat dissipation, and low power consumption.[20] The

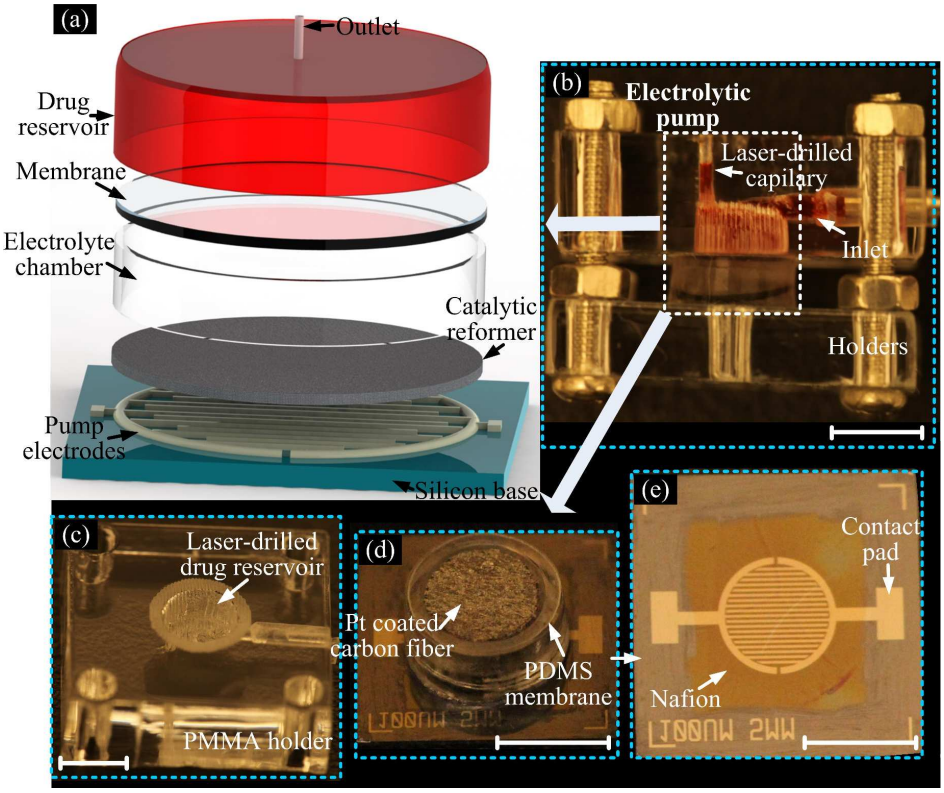

Fig.1 Illustration and photographs of our proposed electrolytic pump: (a) Exploded view of the device showing its major components; (b) Test fixture photo; (c) Drug reservoir cut from PMMA board; (d) Photo of assembled electrolysis actuator including Pt coated carbon fiber mesh; (e) Layout of Nafion coated Pt/Ti electrodes. The scale bars are 5 mm.

actuation of such devices comes from bubbles produced during electrolysis. For example, DI water can be electrolyzed into oxygen and hydrogen, resulting in a gas expansion for pumping. Meng *et al.* have pioneered works optimizing the design of electrolysis-driven actuators[21-22] and attempted to apply electrolytic micro-pumps for chronic ocular disease treatments[23] and anti-cancer drug delivery in mice.[24] However, all of these devices adopted the liquid-drug-in-reservoir (LDR) approach, where maintaining a well-defined dose at the disease site is difficult because the drug concentration in the reservoir varies based on the refilled liquid dilutions.[24] Moreover, long term applications using LDR are hard to achieved once the liquid drug is depleted or the diaphragm achieves its maximum deformation.[21,24] Injecting the drug solution by piercing the reservoir membrane with a syringe needle can extend the functional lifetime of the device,[25-26] which, in turn, increases the concerns about safety, medical cost and extra surgical operations. Further, approximately 40% of new drug candidates possess low solubility in water.[27-28] This low solubility results in low dose density for LDR based drug delivery systems, because low concentration limits the storage of hydrophobic drugs in liquid form, such as docetaxel (solubility of 2.5 μg/L in water).

An alternative approach to LDR is to store the solid drug in a reservoir (SDR). This method provides a solution to the dosage dilemma by increasing the size of the drug reservoir, permitting a long-term application (months or years) because the reproducible dose can be formed by repeatedly dissolving small amounts of the solid drug. Pirmoradi *et al.* introduced a magnetically controlled microfluidic device that is able to pump fluid in and out of the solid drug filling the reservoir.[29-30] The reproducible drug solution can be released by cyclically refilling the reservoir and pumping the dissolved drug liquid, which maintains full pharmacological efficacy for more than one month.[30] The corresponding actuation relies on deforming a magnetic membrane in an applied magnetic field, providing a simplified control strategy. However, this actuation mechanism does not only require an accurate alignment between the magnetic source and the membrane, but it also limits the operation distance. Moreover, exposure to a magnetic field of more than 200 mT over an extended period may harm human health.[31-32]

We previously reported a cyclical pulsed device which integrated a low power and flexible electrolytic pump that used an SDR and had long term dosage and simple control.[33] In this device, an applied DC voltage triggered the electrolytic reaction, inducing bubble generation in the electrolyte chamber. The gas expansion deforms a flat PDMS (polydimethylsiloxane) membrane that is in between the pumping chamber and the drug reservoir, discharging the drug solution out of the reservoir. When power is removed, the fresh liquid automatically refills the reservoir to dissolve more of the remaining solid-form drug. We investigated power-controlled and pulsatile circulating release of a drug substitute with low solubility in a reproducible manner. However, a flat membrane cannot achieve a displacement over its maximum safe deflection, limiting the dosing at each pumping. Therefore, in order to achieve on demand drug release, the ability to improve the number of drug delivery cycles within a given treatment period must be developed. Improving on our previous work, an easily fabricated catalytic reformer was introduced for accelerating the bubble recombination rate, reduces the non-actuation intervals so that the time of each drug delivery cycle is decreased.

In this paper, we added three pieces of platinum (Pt) coated carbon fiber mesh in the electrolyte chamber in order to increase the contact

area between the Pt and electrolysis-induced gas. In this manner, bubble recombination starts immediately once the power is turned off, taking less response time than the normal electrolytic pump without a catalytic reformer. Though added catalytic reformers can increase the recombination rate, they decrease the flow rate during the actuation phase due to simultaneously occurred bubble recombination. Herein, a Nafion coated Pt/Ti electrodes[22] that lead to high current electrolysis efficiency was chosen to compensate for the electrolysis efficiency reduction caused by Pt-coated carbon fiber meshes. The other features of our proposed drug delivery device include: 1) combining a SDR approach with a controllable electrolytic actuation model to extend chronic treatments; 2) lowering the applied power to allow for the possibility of wireless powering,[34-35] which also further miniaturizes the size of the implant; 3). Achieving on demand drug release with a rate that can be accurately achieved by intermittent delivery. We demonstrated the feasibility of our device in terms of stable pumping profiles and drug release rate. Our prototype device is a pivotal next step for treating chronic diseases, such as glaucoma, brain tumors, or narcotics delivery for controlling chronic pain.

2. Design and Theory

Figure 1 illustrates the major components of our proposed drug delivery system, with the corresponding prototype being shown in Fig.1 (b). We assembled the electrolytic pump by tightening PMMA (polymethylmethacrylate) holders for the purpose of repeatable testing, rather than permanently bonding the model components together to reduce the size of the pump. The drug reservoir was drilled in a 6.2-mm thick PMMA board (Moden Glas Acrylic Co., Ltd) using a CO_2 laser cutter (Universal PLS6.75); its dimension include an internal radius of 2.5 mm with a depth of 3.0 mm, providing a maximum volume of 60 µL (Fig.1 c). The pumping chamber was also made of a PMMA loop with a 2.7 mm height (Fig.1 d); its inner radius is 2.6 mm with a wall thickness is 0.6 mm. The pumping chamber is separated from the drug reservoir by a polydimethylsiloxane (PDMS) membrane to avoid electrochemical interaction with drug or bodily fluids. When fabricating the PDMS membrane, we mixed pre-polymer and cross-linker (Dow Corning Sylgard 184) in a ratio of 10:1, and then we spin-coated it on a buffered oxide etched (BoE) silicon wafer after degassing. PDMS film

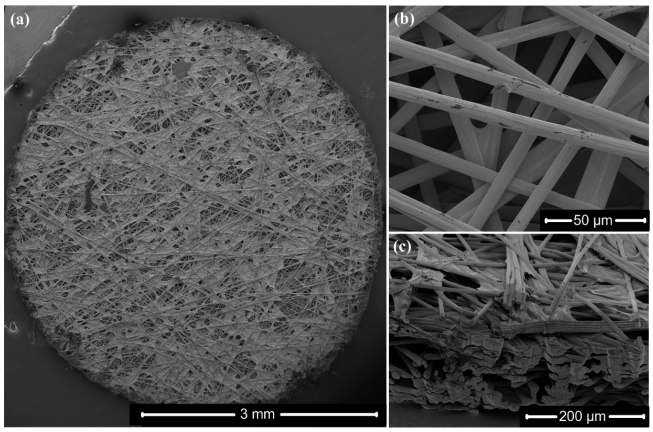

Fig.2 (a) Top SEM view of overall Pt coated carbon fiber mesh, showing the magnified region of the edge from (b) the top view and (c) a cross-sectional view, illustrating the details of the porous structure.

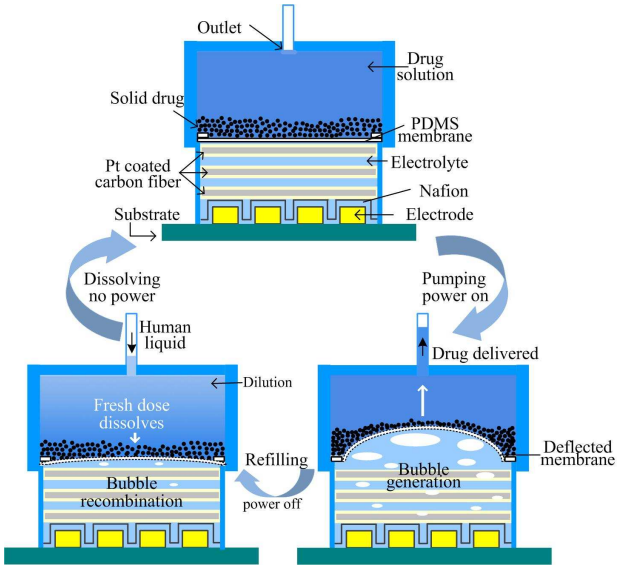

Fig.3 Schematic illustration of the SDR-based drug delivery pump and its "power on and off" mode cyclical operations involving pumping and refilling.

(thickness of 7.9 µm) was cured at 90°C on a hot plate. We included three Pt-coated carbon fiber meshes into the pumping chamber to act as reforming elements in order to improve the cycle time, which is one of the determining factors in our system's ability to provide different dosing profiles. Inter-digitated platinum/titanium (Pt/Ti) electrodes were fabricated on a silicon wafer by a standard photolithography and lift-off processes (Fig.1 e). Titanium functions as an adhesion layer between the silicon surface and Pt. Both the element's width and spacing are 100 µm, which represent an optimal design.[22] The electrodes have a height of 300 nm (thickness ratio: Ti:Pt=1:5), with a Nafion coat of 250 nm to improve the electrolysis-efficiency.

Scanning electron microscope (SEM) images of the Pt coated carbon mesh are depicted in Fig. 2. The porous mesh structure was chosen in order to let the electrolysis-generated bubble pass through and increase the contact area. We selected carbon fiber mesh (porosity: 78% in this work) for the scaffold because it is harmless to human body and will not interact with the electrolyte. In fabrication, we first cut three pieces of identical meshes from a carbon fiber paper, with a round shape to fit the actuator chamber. Thereafter we placed them in a Quorum Q300TD sputtering system. Using a 90 mA ion current, we sputtered Pt to form a layer with a thickness of 100nm. The discs where then turned around, and the same procedure was repeated again, so that both sides and the inner surface were coated with 100nm of Pt. Because each piece of the mesh is very thin (~300 µm), we used multiple pieces in order to further increase the Pt contact area.

The working principle of our proposed drug delivery system is based on a cyclical operation including two phases: pumping at bubble generation and refilling at bubble recombination. The corresponding schematic diagram is illustrated in Fig.3. The first step is to fill the drug reservoir with DI water through the mechanically drilled channel, making the solid drug partly dissolved and prepared for delivery. Once power is applied to the electrodes, an electrolytic reaction starts. The generated bubble pushes the dissolved drug solution outwards due to the deflected PDMS membrane. Power must be removed prior to the membrane reaching

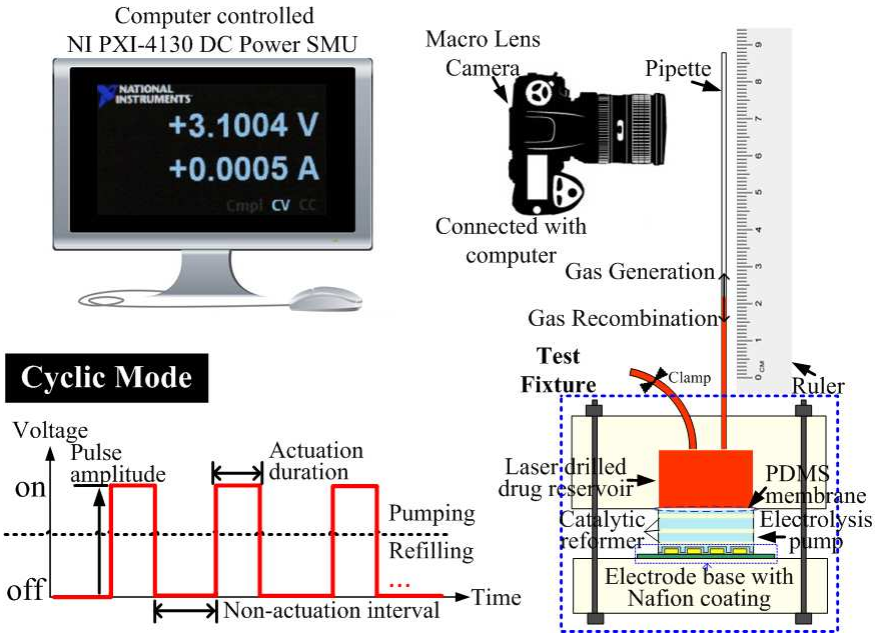

Fig. 4 Schematic diagrams of the experimental setup used to characterize the cyclic operation of our proposed electrolysis-bubble actuated pump.

its maximum displacement. Without applied power, the electrolysis-induced gas (H_2 and O_2) recombines into water. This recombination is assisted by the catalytic properties of the Pt. Pressure decrease in the electrolyte chamber causes the membrane to move downward, sucking external liquid into the drug reservoir to dissolve the rest of the solid-form drug. By repeatedly turning on and off the power, the solid drug can be dissolved and delivered continuously. The amount of drug delivered can be controlled by the number of the actuation cycles, the actuation period, and the wattage of applied power.

3. Experimental results and analysis

3.1 Catalytic reformer function

The electrolytic pump using the catalytic reformer was assembled as depicted in Fig. 1 b; accordingly the experimental measurements for our device is illustrated in Fig. 4. "Power on and off" implements two stages of the cyclic mode: pumping and refilling, respectively. The computer controlled DC power source measure unit (SMU) can supply power to the pump via probes connected to the contact pads of the electrodes. Then the generated electrolysis-bubbles deform the membrane upwards, resulting in the fluid climbing up the pipette, when power is removed, the fluid level decreases due to the bubble recombination in the electrolysis chamber in the presence of Pt coated carbon fiber meshes. We used food coloring in water as the pumped fluid, the colour allowed us to track movements to calculate membrane displacements. A digital camera was used for real-time flow tracking.

The actuation force of the electrolytic pump is provided from the bubbles, including hydrogen (H_2) and oxygen (O_2) induced from dissociation of DI water. Its generation rate increases with an increase of applied current or power.[36] Fig. 5 shows the power controlled flow rates for two different pump versions run under the same experimental conditions: a normal pump with Nafion coating; and one with an added catalytic reformer. The results indicate that the added Pt-coated carbon fiber meshes decrease the electrolysis efficiency and flow rate, because an increased Pt contact area can simultoneously recombine more gas into water even in the electrolysis-generation phase. With increasing applied power, the electrolysis bubble generation becomes faster and more dominant, so the flow rate difference between the pump with and without catalytic reformer becomes smaller.

Labview's vision assistant was used to track the red color flow in order to measure the membrane displacement. Fig. 6 compares the displacement profiles of the two pumps under the same applied power. As analyzed above, the pump using the Pt-coated carbon fiber meshes lowers the flow rate since it brings the effects of competitive bubble recombination. Power was applied until the membrane reached its maximum safe deflection, and then the

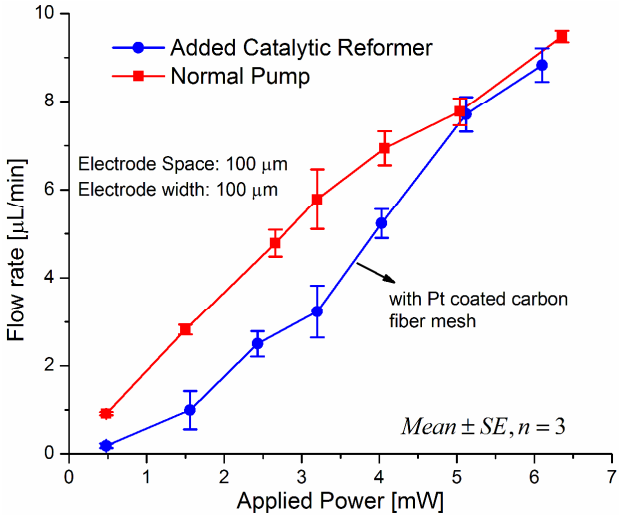

Fig. 5 Power controlled flow rates for the electrolytic pump with and without catalytic reformer (*Mean*±*SE*, *n*=3).

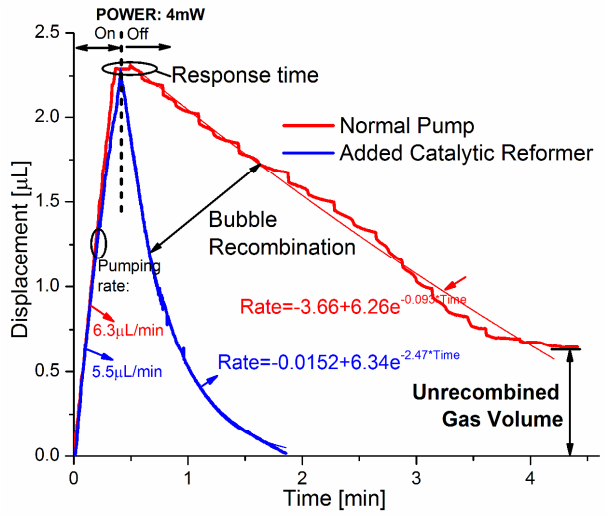

Fig. 6 Real-time membrane displacement of the electrolytic pump with and without catalytic reformers under the same experimental conditions, power of 4 mW was applied and then removed.

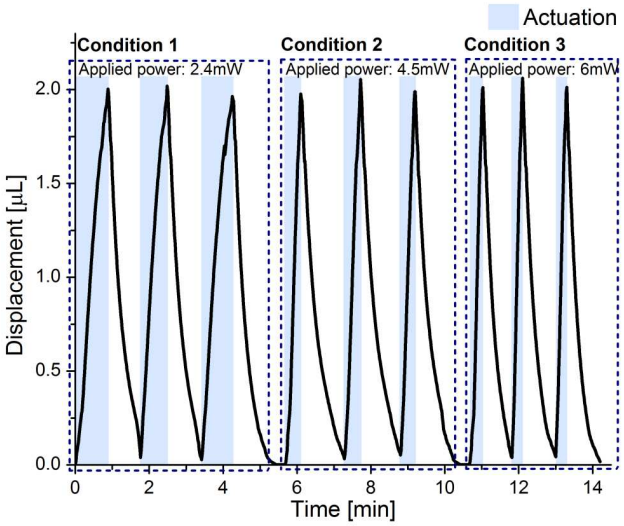

Fig. 7 Cyclical displacement operated with different applied power indicating stable behaviors of electrolysis bubble generation and recombination.

power was removed. The generated bubbles slowly recombined in the normal pump because it only has a Pt electrode and does not use a Pt-coated carbon fiber meshes. As shown in Fig, 6, 72.1% of the pumped volume flows in reverse through the pipette, illustrating a significant portion of unrecombined gas[24] since the Pt contact area is too small. In comparison, using our catalytic reformers, 99.3% of the gas recombines, providing a larger membrane deflection for the next delivery. This improvement in recombination comes at a slight reduction in the efficiency during the power on phase as can be seen from the lower pumping rate (blue) in Fig. 6. However, this faster recombination rate dramatically reduces the period of each cycle, exhibiting a great improvement in cyclical mode.

3.2 Cyclic operations

This subsection evaluates our assembled pump integrated with the catalytic reformers in the cyclical mode. A computer controlled NI DC power source (National Instruments PXI) was used to apply the power to the electrolytic pump. Labview's vision assistant was used to track the movements of the red food coloring solution through the glass capillary in order to characterize the pumping performance of the cyclical mode at different applied powers and actuation frequencies. Fig. 7 shows the profiles of membrane displacement under applied powers of 2.4 mW, 4.5 mW and 6 mW, respectively. The applied power increases lead to a shorter time for pumping due to faster bubble generation. When the power actuation is removed, the electrolysis bubbles immediately start to recombine, causing the red color solution to flow back, which is equivalent to the refilled liquid. The integration of the Pt-coated carbon fiber mesh helps to quickly recombine 2 μL of gas in at about one minute. Actuation conditions 1~3 in Fig. 7 demonstrates the power-controlled and stable abilities of our cyclical pulsed delivery system that uses bubble generation and recombination for pumping and refilling.

In addition to the applied power, the delivery frequency (the cycle numbers over the operation time) is also a critical factor that can determine the amount of drug delivered within a given treatment period. Our proposed device allows for power controlled flow rates and "on demand" delivery frequencies in order to meet the specific

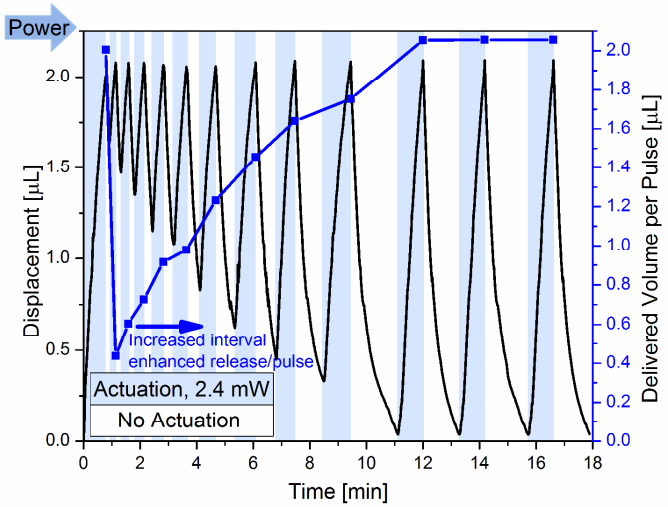

Fig. 8 Membrane displacement operated with different actuation frequencies using a constant power of 2.4 mW.

requirement of drug concentration level, addressing the patients' needs. As an example of our devices functionality, Fig. 8 depicts the relationship between delivery frequency and pumped volume for the cyclic mode when a power of 2.4 mW was used. A higher delivery frequency means a shorter non-actuation interval between actuations, which may not provide sufficient time for full refilling of the reservoir, causing a less fluid to release during subsequent pulses. Decreasing the delivery frequency or increasing the non-actuation interval can enhance the delivered volume at each pumping. In order to obtain a compromise between the delivery frequency and the maximum amount of liquid released during each actuation, adding catalytic reformers is a must. Our Pt-coated carbon fiber meshes can quickly recombine the electrolysis bubble and provide full delivery within short periods, for example, the dose of 2 μL can be prepared in about one minute for the following actuation in this work. Fig. 8 also indicates the stable delivery profile over actuation durations and recombination intervals.

In summary, the addition of our catalytic reformers can nearly recombine all the electrolysis bubble and accelerate the

recombination rate. This effect cannot only provide the maximum achievable displacement for a single delivery, but it also allows for more delivery cycles within a specific treatment time.

3.3 Cumulative drug release

The selection of the solid drug is critical for drug delivery devices that adopt an SDR approach. The basic concept is that the storage is primarily in solid form of which a small portion is dissolved for each successive dose. To ensure that only a small portion is dissolved in each pumping cycle a low solubility drug is required. Overall daily dose is then controlled by the number of fixed volume pumping cycles. A highly soluble drug will be consumed within only a few cycles and dose control will revert back to fine volumetric control like a LDR system. This would eliminate the advantage of the digital like fixed-volume controlled dosing of the SDR approach. In this experiment, we used solvent blue 38 (SIGMA-ALDRICH CO., MO, USA) as a drug substitute to evaluate our device's release performance. The solubility of solvent blue is relatively low, so the solid form can be maintained in a drug reservoir for an extended period, which allows for long-term drug delivery. Solvent blue 38 also allows highly sensitive measurement with detection equipment, such as microliter spectrophotometry (Picodrop Ltd., UK) in this work.

We used the setup depicted in Fig. 9 to measure the release of the chemical substance. An external reservoir filled with 4% w/v bovine serum albumin (BSA) in phosphate buffered saline (PBS, pH 7.4) was used to emulate the human liquid environment (37°C) to which the drug is delivered. This solution was considered to be a suitable model of physiological fluid[30] and widely used for in-vitro release tests [4, 17, 30]. A magnetic stirring bar was put into the external reservoir for accelerating the drug diffusion uniformly into the external liquid when the stirrer (Advanced Multi-position Stirrer, Henry Troemner LLC, USA) started to work. It is an idealized testing model, where cell absorptions are not taken into account. The electrical wires were soldered to the electrodes of the pump so that the DC power could power the device. We carefully placed the solvent blue 38 in powdered form on top of the PDMS membrane in advance. Then the PBS solution was injected in the drug reservoir through a laser-drilled inlet (see the insert of Fig. 9)

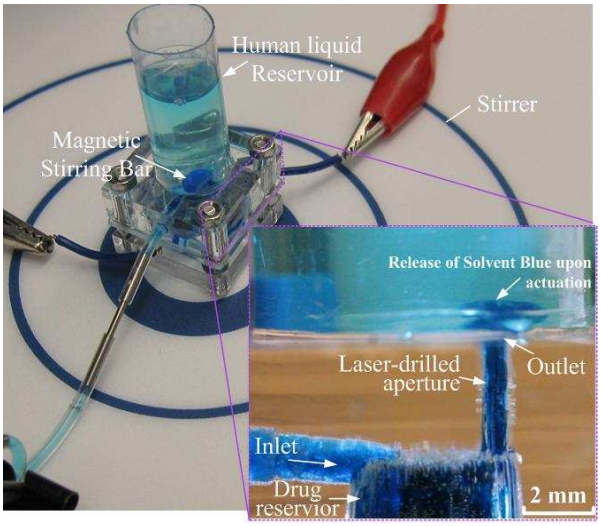

Fig. 9 Experimental apparatus of drug delivery, side view of device depicts release of solvent blue into external solution upon electrolysis bubble actuation.

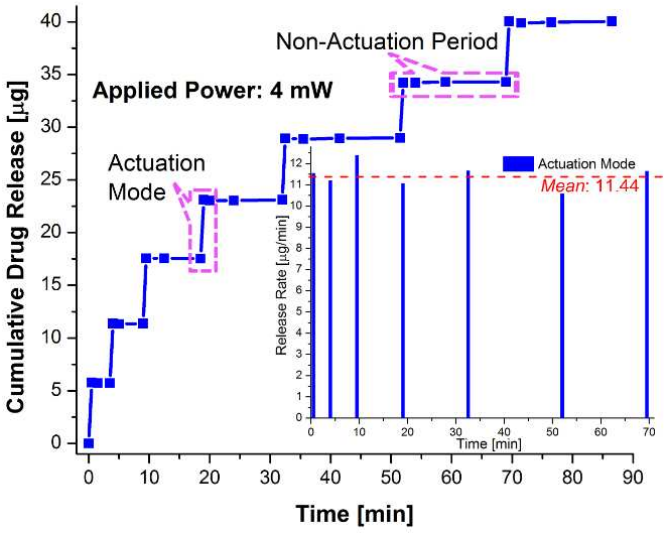

Fig.10 Intermittent release of solvent blue 38 from the pump to the external reservoir by applied power of 4 mW. After each pumping a period of delivery is followed with non-actuation mode. Released solvent blue 38 was cumulated by a series of actuations.

after the pump was assembled. We clamped the inlet afterwards, so that the laser-drilled outlet was the only channel used for pumping and refilling.

As we already stated, the drug solution was pumped by electrolysis-bubble generations and its volume corresponds to the displacement caused by the membrane deflection. The inset of Fig. 9 demonstrates the released drug upon electrolytic actuation. The electrolytic reaction is reversible in the presence of Pt, so bubble recombination occurred when the applied power was removed. The external liquid refilled the drug reservoir and mixed with the previous drug solution to dissolve fresh drug and achieve concentration equilibration for the next dose.

In this experimental test, about 25% of the volume of the drug reservoir was used to store 3 mg of the solvent blue 38. We fixed the applied power at 4 mW, and the actuation time was 30 seconds for each delivery cycle. We used microliter spectrophotometry to measure the concentration change of the liquid in the external reservoir at the end of each delivery. Accordingly, the amount of each release with and without actuation was determined as shown in Fig. 10. The continuous power on-off operations provided a consistent drug release for multiple pulses over 90 minutes with a stable release rate of 11.44 ± 0.56 μg/min (Mean ± SD) during each actuation cycle of 30 seconds (the inset of Fig. 10). Two factors account for this stable dosing: Firstly, the volume ratio between the newly refilled liquid and drug reservoir was ~2 μL:60 μL. This ratio reduces the impact on the overall concentration inside the drug reservoir; Second, fresh solid drug dissolves into the dilution within the non-actuation period in order to form a new concentration equilibration close to the previous one. The profiles of the drug release demonstrate the feasibility and stability of our device.

In this work, diffusion-based drug release during the non-actuation period was rare due to a short non-actuation interval (from 2 minutes to 10 minutes in Fig. 10). However, for the long term, its effects cannot be ignored. We did an independent test for six days, and we measured that 20 μg of solvent blue 38 diffused into the external liquid. Therefore the average diffusion rate over the course of these

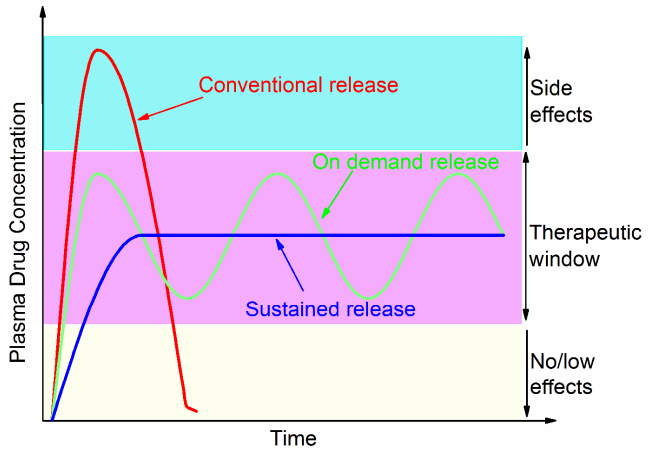

Fig.11 Illustration depicting therapeutic window and different releasing profiles.

six days was 2.3 ng/min. In order to prevent such diffusion, a variety of valves can be developed in conjunction with our device in order to avoid these effects over long-term usage.

Finally, the drug storage density can be maximized to 50% or even more (25% in this work), which in turn increases the drug storage. For those special diseases that needs less daily drug dose, such as posterior uveitis, a fluocininolone acetonide implant can be used, which releases the drug at a rate of 0.6 μg/day for treating.[37] The daily dose of approximately 0.001 μg to 10 μg of ophthalmic delivery were proposed by taxane-cobalamin bio-conjugates.[38] Even 3 mg of drug storage can provide 10 μg of daily dose over 300 days or 0.6 μg of daily dose over 5000 days. The frequency of replacement of our device is far less than the previously reported new liquid drug refilled frequency of 33 days or 3 months,[23] which makes it ideal for long-term applications.

4. Discussion

Fig. 11 illustrates the concentration profiles of the released drug depending on various working mechanisms. Conventional drug delivery methods are usually not controllable, resulting in unstable biological effects to patients. Above the effective therapeutic range, the drug concentration brings side effects at the onset of release, while it drops to inefficient levels overtime. In order to maximize the efficacies of the delivered drug and to minimize the negative influence at the disease site, the drug concentration must be strictly controlled within the therapeutic window. Different than conventional methods, controlled drug delivery systems can optimize pharmacological effects within the effective therapeutic range and reduce the possibilities of unreasonable concentration-induced toxicity. Controlled methods are generally classified as two types according to their release kinetics: sustained release and "on-demand" release.

Sustained mechanisms can maintain a stable concentration within the therapeutic range, but they require constant actuation for delivering the drug continuously. Devices using this method usually contain a fixed volume of drug, and its release is constant with time. A drawback of these devices is that once the device is implanted, changing the drug, concentration level or the rate of release is difficult. An osmotic pump[39] is a popular example that can provide continuous and slow drug infusion, because its actuation mainly relies on the diffusion between two solutions with different solute concentrations, and the process of such a drug delivery is "passively controlled" at the time of manufacture. Though Cai *et al.*[40] developed a drug release "switch on and switch off" model by changing the direction of external magnetic field, the release of DNA and vitamin B2 is still based on slow osmotic flow through a porous membrane.

In order to accomplish "actively controlled" drug delivery with a predicable release dose or rate at the disease site, the external stimulus-responsive devices must be developed. For example, a telemetry controlled microchip implant can provide pulsatile release of polypeptide leuprolide over six months in dogs.[41] In this paper, we adopted an on demand drug delivery model by using a power-controlled electrolytic pump. This system can release various dosages of drug by intermittent delivery and achieve a pulsed profile of concentration based on the release rate and time, therefore, our devices is well suited for those circumstances when the physiological conditions occasionally change, requiring varying dose during use.

Moreover, biofouling is an issue in long-term implantable devices.[42] Strategies for mitigating biofouling involve sustained release of biological response modifiers (BRMs) [43-44] and anti-fouling membrane coatings [45] and can be implemented in future versions of the devices that are intended for in vivo testing. But this work presents a proof of concept for an electrolytically powered SDR system and as a result has not yet incorporated any strategies to deal with biofouling.

Finally, our device can be actuated by external power, for example, a wireless power transfer control unit, where a patient's external unit can control the release by adjusting the applied power strength and actuation interval according to the drug concentration requirements. The ability to adjust the dose per pulse and the frequency of the delivery allows for a highly tailorable dosing profile that can be adapted to changing treatment needs by just changing the program in the external powering unit.

5. Conclusions

This work investigated an on-demand electrolysis-driven pump intended for an accurate and controlled drug delivery system. Various release dosages and rates can be achieved by adjusting the applied power, such that it meets the concentration requirements at the disease site. An SDR approach was adopted, which is appropriate for long-term therapeutic treatments via the cyclically pulsed mechanism. This method uses cyclical power between on and off, dissolving a solid-form drug in human liquid during the bubble recombination phases, and forming reproducible drug solution for delivery at bubble generation phases.

The other key advantage over existing electrolytic pumps is that our device includes the Pt-coated carbon meshes in the actuator chamber. These reforming elements not only improve the recombination rate, but they lead to a faster drug release cycle than the normal device. The Pt-coated carbon meshes aid in fully combining the generated gas into water, thus increasing the membrane displacement for the next delivery. The drug concentration level is mainly a function of the delivery frequency and the volume of each delivery. Therefore, shorter pulsed periods mean that more cycles of drug release can be achieved within a given time. In other words, a wider dose range within a specific therapeutic period can be guaranteed, so that drug concentration can be controlled according to the current requirements of treatment.

A low aqueous solubility drug substitute, solvent blue 38, was used to characterize our device. Our experimental results indicate that a consistent release rate of 11.44 ± 0.56 μg/min was achieved in each actuation under an applied power of 4 mW. Because the concentration in the drug reservoir remains

constant (close to the saturation state) before each delivery, the resulting release dose can be calculated using the drug's saturation and the pumped volume. The cumulative release of multiple pulses demonstrates the stability and feasibility of our proposed system.

References

1 Meng Ellis, and Tuan Hoang, Advanced drug delivery reviews, 2012, **64**, 1628-1638.
2 D.C. Metrikin, R. Anand, Curr. Opin. Ophthalmol., 1994, **5**, 21–29.
3 H. F. Edelhauser, C. L. Rowe-Rendleman, M. R. Robinson, D. G. Dawson, G. J. Chader, H. E. Grossniklaus, K. D. Rittenhouse, C. G. Wilson, D. A. Weber, B. D. Kuppermann, K. G. Csaky, T. W. Olsen, U. B. Kompella, V. M. Holers, G. S. Hageman, B. C. Gilger, P. A. Campochiaro, S. M. Whitcup and W. T. Wong, Invest. Ophthalmol. Visual Sci, 2010, **51**, 5403–5420.
4 Y. Li, D. Hong Linh Ho, B. Tyler, T. Williams, M. Tupper, R. Langer, H. Brem and M. J. Cima, J. Controlled Release, 2005, **106**, 138–145.
5 D.A. LaVan, T. McGuire, R. Langer, Small-scale systems for in vivo drug delivery, Nat. Biotechnol. 2003, **21 (10)**, 1184– 1191.
6 K. E. Uhrich, S. M. Cannizzaro, R. S. Langer and K. M. Shakesheff, Chem. Rev., 1999, **99**, 3181–3198.
7 A.Gopferich, Biomaterials, 1996, **17**, 103–114.
8 R. Yoshida, Curr. Org. Chem., 2005, **9**, 1617–1641.
9 Saltzman, W. M. & Olbricht, W.L., Nat. Rev. Drug. Discov. 2002, **1**, 177–186.
10 D. J. Laser and J. G. Santiago, J. Micromech. Microeng., 2004, **14(6)**, 35–64.
11 M. Staples, Wiley Interdiscip. Rev.: Nanomed. Nanobiotechnol., 2010, **2**, 400–417.
12 B. Ziaie, A. Baldi, M. Lei, Y. Gu and R. A. Siegel, Adv. Drug Delivery Rev., 2004, **56**, 145–172.
13 Tao, S.L. & Desai, T.A., Adv. Drug Deliv. Rev., 2003, **55**, 315–328.
14 Teymoori, M. M., & Abbaspour-Sani, E., Sensors and Actuators A: Physical, 2005, **117**, 222-229.
15 J. Kan, Z. Yang, T. Peng, G. Cheng, and B.Wu, Sens. Actuators A, Phys., 2005, **121(1)**, 156–161.
16 S. Santra, P. Holloway, and C. D. Batich, Sens. Actuators B, Chem., 2002, **87**, 358–364.
17 J. T. Santini, M. J. Cima and R. Langer, Nature, 1999, **397**, 335–338.
18 Su Yu Chuan, and Liwei Lin, Journal of Microelectromechanical Systems, 2004, **13**, 75-82.
19 Stroock, Abraham D., Marcus Weck, Daniel T. Chiu, Wilhelm TS Huck, Paul JA Kenis, Rustem F. Ismagilov, and George M. Whitesides, Physical review letters, 2000, **84**, 3314-3317.
20 D. A. Ateya, A. A. Shah, and S. Z. Hua, Rev. Sci. Instrum., 2004, **75(4)**, 915–920.
21 Li, Po-Ying, Roya Sheybani, Christian A. Gutierrez, Jonathan TW Kuo, and Ellis Meng, J. MEMS., 2010, **19**, 215-228.
22 Sheybani, Roya, and Ellis Meng, Journal of Microelectromechanical Systems, 2012, **21**, 1197-1208.
23 Li, Po-Ying, Jason Shih, Ronalee Lo, Saloomeh Saati, Rajat Agrawal, Mark S. Humayun, Yu-Chong Tai, and Ellis Meng, Sensors and Actuators A: Physical, 2008, **143**, 41-48.
24 Gensler, Heidi, Roya Sheybani, Po-Ying Li, Ronalee Lo Mann, and Ellis Meng, Biomedical microdevices, 2012, **14**, 483-496.
25 R. Lo, P.-Y. Li, S. Saati, R. Agrawal, M. Humayun and E. Meng, Lab on a Chip, 2008, **8**, 1027-1030.
26 R. Lo, P. Y. Li, S. Saati, R. Agrawal, M. Humayun and E. Meng, Biomed. Microdevices, 2009, **11**, 959–970.
27 T. Bo, G. Cheng, J. C. Gu, and C. H. Xu, Drug discovery today, 2008, **13(13)**, 606-612.
28 W. Hywel D., N. L. Trevaskis, S. A. Charman, R. M. Shanker, W. N. Charman, C. W. Pouton, and C. J. H Porter, Pharmacological reviews, 2013, **65(1)**, 315-499.
29 Pirmoradi, Fatemeh Nazly, John K. Jackson, Helen M. Burt, and Mu Chiao, Lab on a Chip, 2011, **11**, 3072-3080.
30 Pirmoradi, Fatemeh Nazly, John K. Jackson, Helen M. Burt, and Mu Chiao, Lab on a Chip, 2011, **11**, 2744-2752.
31 Miyakoshi, Junji, *et al.* Journal of radiation research, 2000, **41(3)**, 293-302.
32 Lai, Henry, and Narendra P. Singh, Environmental health perspectives, 2004, **112(6)**, 687-694.
33 Yi, Y., Buttner, U., & Foulds, I. G. MicroTAS., 2012, 527-529.
34 T. B. Tang, S. Smith, B. W. Flynn, J. T. M. Stevenson, A. M. Gundlach, H. M. Reekie, A. F. Murray, D. Renshaw, B. Dhillon, A. Ohtori, Y. Inoue, J. G. Terry and A. J. Walton, IET Nanobiotechnol., 2008, **2**, 72–79.
35 Yi, Y., Buttner, U., Fan, Y. Q., Foulds, I. G. International Journal of Circuit Theory and Applications, 2014, ahead-of-print.
36 J. Xie, Y. Miao, J. Shih, Q. He, J. Liu, Y. C. Tai, and T. D. Lee, Anal. Chem., 2004, **76**, 3756–3763.
37 J. Glenn, R. M. McCallum, B. Branchaud, C. Skalak, Z. Butuner, and P. Ashton, Ophthalmology, 2005, **112(7),** 1192-1198.
38 J. R. Gebhard and D. Patel, *US Pat.*, 2010, 12/56,780.
39 Herrlich, Simon, *et al*., Advanced drug delivery reviews, 2012, **64(14)**, 1617-1627.
40 K. Cai, Z. Luo, Y. Hu, X. Chen, Y. Liao, L. Yang and L. Deng, Adv. Mater., 2009, **21**, 4045–4049.
41 J. H. Prescott, S. Lipka, S. Baldwin, N. F. Sheppard, J. M. Maloney, J. Coppeta, B. Yomtov, M. A. Staples and J. T. Santini, Nat. Biotechnol., 2006, **24**, 437–438.
42 V. Santhisagar, I. Tomazos, D. J. Burgess, F. C. Jain, and F. Papadimitrakopoulos, Biosensors and Bioelectronics, 2010, **25(7)**, 1553-1565.
43 B. Upkar, R. Sura, F. Papadimitrakopoulos, and D. J. Burgess, Journal of diabetes science and technology, 2007, **1(1)**, 8-17.
44 O. Yoshinori, U. Bhardwaj, F. Papadimitrakopoulos, and D. J. Burgess, Journal of diabetes science and technology, 2008, **2(6)**, 1003-1015.
45 G. Evin, D. Nagesha, S. Sridhar, and M. Amiji, Advanced drug delivery reviews, 2010, **62(3)**, 305-315.